ESC European Society of Cardiology

Europace (2023) **25**, 748–755
https://doi.org/10.1093/europace/euac191

BASIC SCIENCE

Differential effect of high-frequency electroporation on myocardium vs. non-myocardial tissues

Yonatan Moshkovits [1†], Dvora Grynberg [2†], Eyal Heller [1,2], Leonid Maizels [1,2], and Elad Maor [1,2*]

[1]Leviev Heart Center, Sheba Medical Center, Derech Sheba 2, Ramat-Gan 52621, Israel; and [2]Sackler School of Medicine, Tel Aviv University, Tel-Aviv 39040, Israel

Received 29 August 2022; accepted after revision 30 September 2022; online publish-ahead-of-print 28 October 2022

Aims Pulsed-field ablation (PFA) is an emerging non-thermal ablation method based on the biophysical phenomenon of electroporation. Data on PFA cardiac selectivity nature and tissue-specific thresholds are lacking. We aim to compare the *in vivo* differential effect of high-frequency irreversible electroporation (HF-IRE) protocols on various tissues.

Methods and results Twenty-three Sprague-Dawle rodents were allocated into three different protocols of 300, 600, and 900 V, respectively, while delivering twenty 100 µs bursts of a 150 kHz biphasic square wave to five tissues; cardiac muscle, skeletal muscle, liver, carotid artery and sciatic nerve. Lesions were evaluated quantitatively by histologic analysis and by morphometric evaluation. There were eight, seven and eight animals in the 300, 600, and 900 V protocols, respectively. High-frequency electroporation protocols showed a graded effect on myocardial tissue with larger lesions in the 900 V protocol compared with the other two protocols as demonstrated by width ($P = 0.02$), length ($P = 0.01$) and fibrosis ratio ($P = 0.001$). This effect was not observed for other tissues with attenuated degree of damage. No damage to the carotid artery was observed in all protocols. Partial damage to the sciatic nerve was observed in only two samples (25%) in the 600 V group and in one sample (14.3%) in the 900 V group.

Conclusion Electroporation effect is tissue-specific such that myocardium is more prone to electroporation damage compared with neural and vascular tissues. Our results suggest no neural or vascular damage with using a low-amplitude HF-IRE protocol. Further investigation is warranted to better identify other tissue-specific thresholds.

* Corresponding author. Tel: +972546444022; fax: +97246385777. *E-mail address*: elad.maor@sheba.health.gov.il
† These authors contributed equally to this work.

Graphical Abstract

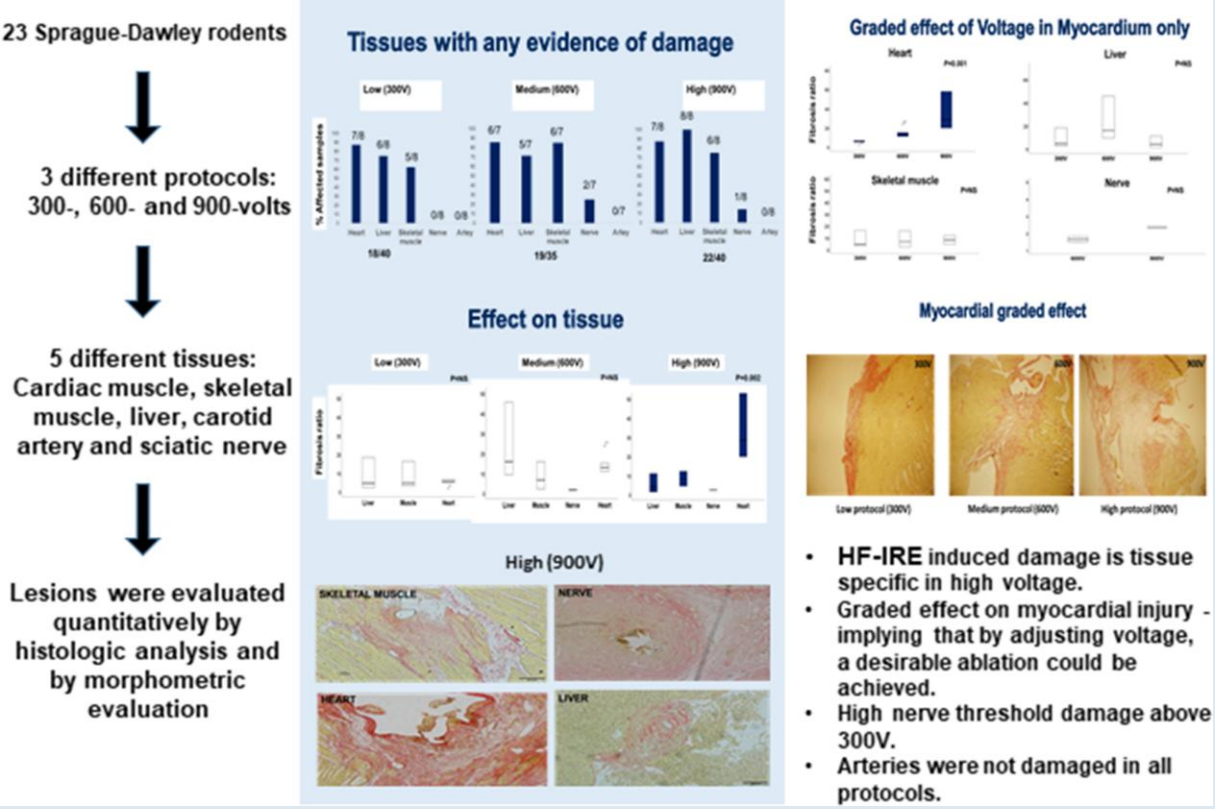

Keywords Electroporation • Cardiac selectivity • Pulsed-field ablation • High-frequency electroporation

What's new?

- Electroporation effect is tissue-specific such that myocardium is more prone to electroporation damage compared with hepatic, vascular, and neural tissues.
- Our results suggest no neural or vascular damage with using a low-amplitude high-frequency electroporation protocol.
- Irreversible electroporation protocol details are critical when planning ablation in such that specific protocols can allow higher specificity with selective damage to cardiac tissue.
- Our findings further establish the safety, specificity, and feasibility of this innovative method and future application.

Introduction

Atrial fibrillation (AF) is a common arrhythmia and its prevalence is expected to increase.[1] Contemporary data suggests that catheter ablation is superior to antiarrhythmic medications in both controlling AF and improving quality of life.[2,3] Catheter ablation aims to electrically isolate and modified the foci of ectopic beats that triggers AF and is focused on pulmonary vein isolation.[2,4] Common ablation techniques utilize thermal damage either by radiofrequency ablation (RFA) or cryoablation with RFA been the most frequently used.[2,5] Although effective, thermal-based catheter ablation has several limitations. First, controlling the extent of thermal injury and damage to nearby organs is limited and therefore extreme temperatures are usually avoided which can lead to non-continuous fibrotic lesions and limited efficacy.[6] Second, in order to avoid pulmonary vein stenosis, thermal ablation within the pulmonary veins, the source of the arrhythmia, is avoided and instead implemented in the atrium, thus impairing ablation effectiveness and increasing the extent of myocardial damage.[3] Additionally, thermal ablation induces non-specific damage with denaturation of proteins, necrotic cell death and inflammatory response that extends to the epicardial fat.[7] Moreover, oesophageal perforation (mainly with RFA) and phrenic nerve palsy (with cryoablation) are rare but serious complications resulting from undesired transfer of the thermal energy to tissues adjacent to the heart.

Irreversible electroporation (IRE), or pulsed-field ablation (PFA) is an emerging non-thermal ablation modality that utilize the induction of short, high-voltage electrical pulses enabling cell membrane pores formation, increased membrane permeability and apoptosis.[8] Irreversible electroporation effectiveness and safety is mainly attributed to its non-thermal nature and the fact that it induces apoptosis rather than necrosis, leading to faster healing and reduced inflammatory response in the affected area.[9] Pre-clinical IRE studies successfully demonstrated the induction of transmural pulmonary vein lesions without pulmonary vein stenosis,[10] and selective ablation of Purkinje fibres with no evidence of myocardial damage.[11] Furthermore, recent PFA clinical trials demonstrated promising results with high success rate and low risk of procedural complications.[12–14] Nevertheless, standard monophasic PFA protocols are limited by collateral neuromuscular stimulus, thus

requiring sedation or general anaesthesia and muscle-relaxants.[15] Modified IRE protocols, such as high-voltage high-frequency electroporation (HF-IRE), may induce scar tissue with minimal nerve stimulation[16,17] enabling a safe alternative to thermal ablation or standard PFA.

While pre-clinical data suggest that electroporation may effectively target myocardial tissue while sparing adjacent nerves and arteries, specific tissue thresholds are unknown and the clinically used electroporation protocols are not disclosed by the industry.[11–13,18,19] Therefore, this study aims to examine the differential effect of HF-IRE on various tissues.

Methods

Electroporation equipment and protocols

High-frequency high-voltage protocols were applied using a custom-made generator, based on an H bridge circuit consisting of four N and P channels MOSFET[17] (*Figure 1*). Two electrodes configurations were used in the experiments (*Figure 1*). The first included a two 3 mm length needle electrodes at a distance of 5 mm. The second configuration used a two-clamp electrodes (0.5 mm in diameter) with 0.5 cm inter-electrode distance. The custom-designed pulse-generator, pulse delivery parameters including a comparison between standard monophasic and HF-IRE and a computer-based simulation of the electric field distribution during cardiac ablation were previously well characterized.[17] As previously demonstrated by the computer-based simulation,[17] the electric field intensity was between 700 and 900 V/cm proximal to the needles with rapidly decay toward the centre of the domain.

Three different HF-IRE protocols were implemented, differing in peak amplitude; 300 V (600 V/cm), 600 V (1200 V/cm) and 900 V (1800 V/cm) (*Table 1*). All protocols used 100 µs bursts of a 150 kHz biphasic square wave with repetition rate of 1 burst/s and the same number of bursts ($n = 20$).

Documentation of voltage and current during cardiac ablation was performed using a digital oscilloscope TBS2000 series (Tektronik).

Animal model

This study was approved by the ethical committee of the Chaim Sheba Medical Center (approval number 1171-18-ANIM). Twenty-five female Sprague–Dawley rats (Envigo LMS Ltd) were used in the current study. All procedures were performed under sterile conditions. The *in vivo* experiment included HF-IRE ablation of five different tissues in five separate locations—cardiac muscle, skeletal striated muscle (quadriceps), liver, carotid artery and sciatic nerve. Cardiac muscle ablation was performed using a left thoracotomy with two needle electrodes (3 mm in length and 0.5 cm inter-electrode distance) as previously described.[17] Liver ablation was carried out using two-clamp electrodes with 0.5 mm in diameter and 0.5 cm inter-electrode distance, placed between the left hepatic lobe as previously described.[20] Skeletal striated muscle and sciatic nerve ablation was carried out using a transverse incision of the lower limb with the implementation of two-clamp electrodes with 0.5 mm in diameter and 5 mm width between them, placed between the left quadriceps and the sciatic nerve. Carotid artery ablation was carried out using two-clamp electrodes with 0.5 mm in diameter and 0.5 cm inter-electrode distance, placed between the right sternocleidomastoid and the carotid artery as previously described.[21] Following the procedures, all surgical incisions were sutured, and animals were extubated and placed back to the animal facility. Animals were sacrificed after 14 days of follow-up. Tissues were perfused with 4% formaldehyde. Cardiac muscle, carotid artery, and sciatic nerve were sliced into three horizontal cuts, perpendicular to the longitudinal axis and adjacent to the ablation site, while the remaining tissues were sliced into three longitudinal cuts. Haematoxylin & Eosin staining and picrosirius stains for fibrosis were used. Slides were digitally stored using a digital microscope. Measurements (length and width) were carried out using CellSense Imagine software (Olympus®) while the extent of fibrosis was evaluated with Fiji software (ImageJ®) (*Figure 2*). Evaluation of damage was performed using measurements of width, length, and degree of fibrosis as observed after picrosirius staining. Slides with the most extensive damage were selected and analyzed. Degree of fibrosis is presented by fibrosis ratio, calculated by the ratio of the percent of fibrosis in the scar divided by percent of fibrosis in healthy tissue, as measured with the Fiji software.

Statistical analysis

Measurements are presented as average and standard deviation. Protocols were compared by one-way ANOVA between peak amplitudes for fibrosis ratio, length, and width. Similarly, a comparison between tissues for the same peak amplitude was conducted using one-way ANOVA for fibrosis ratio, length, and width. Statistical analyses were performed using SPSS version 34.0. Statistical significance was defined as P-value < 0.05.

Results

A total of 25 female Sprague–Dawley rats (Envigo LMS Ltd) were primarily used in this study, of them 23 survived the surgical procedure and follow-up period (*Table 1*). There were eight, seven, and eight animals in protocol Groups 1, 2, and 3, respectively. Of 345 histological slides evaluated, 177 (51.3%) slides showed observable damage and 59 (17.1%) demonstrated significant damage and were included in the final analysis. The histologic appearance of an untreated healthy tissue compared with the ablated scarred tissue are presented in *Figure 3*. During the procedure, minimal muscle contractions were observed with the exception of sciatic nerve and skeletal striated muscle ablation, where significant collateral contraction of the affected limb was noted. Following

Figure 1 Equipment description and configuration; (left) a custom-made generator based on an H bridge circuit consisting of four N and P channels MOSFET. The generator enables a maximal output voltage of 1100 V, at a frequency range of 75–150 kHz with burst duration between 100 and 200 µs. (Right) Two needle electrodes (top) with 3 mm in length and with 5 mm distance between them and (bottom) two-clamp electrodes (0.5 mm in diameter) with 0.5 cm inter-electrode distance.

Table 1 Effect of HF-IRE protocols on tissue damage as quantify by length, width, and fibrosis ratio

Tissue	Protocol (V)	Total samples *N*	Affected samples *N* (%)	Length (μM), Mean ± SD	Width (μM), Mean ± SD	Fibrosis ratio ± SD	*P*-value[a]		
							Length	Width	Fibrosis ratio
Cardiac muscle	300	8	7 (87.5)	1352.0 ± 955.9	428.3 ± 315.0	5.5 ± 1.9	0.01	0.02	0.001
	600	7	6 (85.7)	872.2 ± 414.0	934.2 ± 914.6	13.8 ± 5.1			
	900	8	7 (87.5)	2680.6 ± 1333.5	1376.3 ± 862.5	38 ± 23.9			
Liver	300	8	6 (75)	747.9 ± 542.2	417.6 ± 333.7	9.6 ± 10.2	0.2	0.4	0.2
	600	7	5 (71.4)	1698.2 ± 1087.8	703.1 ± 402.4	22.7 ± 27.2			
	900	8	8 (100)	1282.3 ± 709.3	604.1 ± 286.2	6.7 ± 7.3			
Skeletal striated muscle	300	8	5 (62.5)	563.2 ± 267.6	240.1 ± 95.6	9.6 ± 11.3	0.1	0.3	0.9
	600	7	6 (75)	1411.1 ± 904.9	608.9 ± 580.9	7.8 ± 8.3			
	900	8	6 (75)	1182.3 ± 502.6	516.4 ± 374.2	8.2 ± 3.9			
Sciatic nerve	300	8	0 (0)	–	–	–	0.9	0.2	0.2
	600	7	2 (25)	1273.5 ± 119.9	399.2 ± 272.0	1.6 ± 0.2			
	900	8	1 (14.3)	1290.3	1341.7	2.3			
Carotid artery	300	8	0 (0)	–	–	–	–	–	–
	600	7	0 (0)	–	–	–			
	900	8	0 (0)	–	–	–			

μM, micrometer; HF-IRE, high-frequency electroporation.
The following table present tissue damage quantify by measurements of length (μM), width (μM), and fibrosis ratio. The table also describes number of affected samples with any observable damage for the different protocols. Protocols are differing in peak amplitude; 300 V (600 V/cm), 600 V (1200 V/cm), and 900 V (1800 V/cm).
[a]One-way ANOVA results describes the comparison between protocols in the same tissue.

the acute experiment, all animals survived the 14 days follow-up with no significant morbidity.

Representative waveforms documented during cardiac ablation is demonstrated in supplementary material online, *Figure S1*. The peak to peak voltage was ∼1070 V and average current peak was ∼0.8 A.

Differential effect on tissue

Damage to hepatic tissue, quantified using the extent of tissue fibrosis, was observed in six (75%), five (71.4%), and eight (100%) samples in Protocols 1, 2, and 3, respectively. Skeletal muscle damage was noted in five (63%), six (75%), and six (75%) of samples in Protocols 1, 2, and 3, respectively. In contrast to liver and striated muscle, sciatic nerve damage was only observed in two samples (25%) in the 600 V group with a mean length of fibrosis of 1274 ± 120 μM and in one sample (14%) in the 900 V group with length of 1290 μM. No apparent damage to the carotid artery was observed in all three protocols. Myocardial tissue exhibited the most extensive damage in almost all protocols with seven (88%), six (88%), and seven (88%) of the samples affected protocols 1, 2, and 3, respectively.

Within the 300 V protocol group, myocardial damage was more pronounced compared with skeletal and hepatic tissue with significantly wider lesions (mean width 428 ± 315 μm vs. 240 ± 96 μm and 418 ± 334 μm, respectively, $P = 0.04$) and non-significant longer lesions (mean length 1352 ± 956 μm vs. 563 ± 268 μm and 748 ± 542 μm, P = NS) and fibrosis ratio (mean ratio 6 ± 2 vs. 10 ± 11 and 10 ± 10, P = NS). Within the 600 V group, liver tissue showed the most extensive damage according to fibrosis length (mean length 1698.2 ± 1087.8 μm) and fibrosis ratio (mean ratio 22.7 ± 27.2 μm) with non-significant difference between liver, skeletal and myocardial tissues. Most importantly, in the 900 V protocol group, one-way ANOVA showed significant differences in tissue damage between myocardial tissue and both skeletal muscle and liver tissues in length (2681 ± 1334 μm vs. 1182 ± 503 μm and 1282 ± 709 μm, respectively; $P = 0.03$) width (1376 ± 863 μm vs. 516 ± 374 μm and 604 ± 286 μm, respectively; $P = 0.001$) and fibrosis ratio (38 ± 24 vs. 8 ± 4 and 6.7 ± 7.3, respectively; $P = 0.002$).

Differential effect of voltage amplitude

Most of the affected samples were observed following the highest voltage protocol with 22 of 40 (55%) samples demonstrating substantial tissue damage, as compared with 19 of 35 (54%) in the 600 V protocol and only 18 of 40 (45%) in the lower 300 V protocol. *Figure 4* presents histologic appearance of the ablated cardiac tissue for increasing voltage protocols. As demonstrated in *Table 1*, damage was observed in the majority of samples in all protocols. As predicted, cardiac tissue fibrosis was greater in the 900 V protocol as compared with lower voltage protocols (*Figures 4* and *5*, *Table 1*). Mean width for myocardial lesions was 429 ± 315, 694 ± 493 and 1348 ± 892 μm for the low-, medium-, and high-voltage protocols, respectively. Myocardial tissue damage demonstrated a positive correlation with voltage in such that tissue injury was more noticeable in the 900 V protocol as compared with the other protocols (P values of 0.01, 0.02, and 0.001 for length, width, and fibrosis ratio, respectively). No significant differences in tissue damage were found between the low- and medium-voltage protocols with respect to myocardial tissue. In liver tissue on the other hand, the extent of tissue damage did not correlate with voltage. Hence, the medium-voltage protocol resulted in the greatest tissue damage, but such differences between the protocols did not reach statistical significance in any of the three damage parameters evaluated. Similar findings were observed with respect to skeletal muscle demonstrating no graded effect between protocols in all tissues.

Discussion

The main finding of the current study is that myocardial tissue is more sensitive to electroporation induced damage compared with vascular,

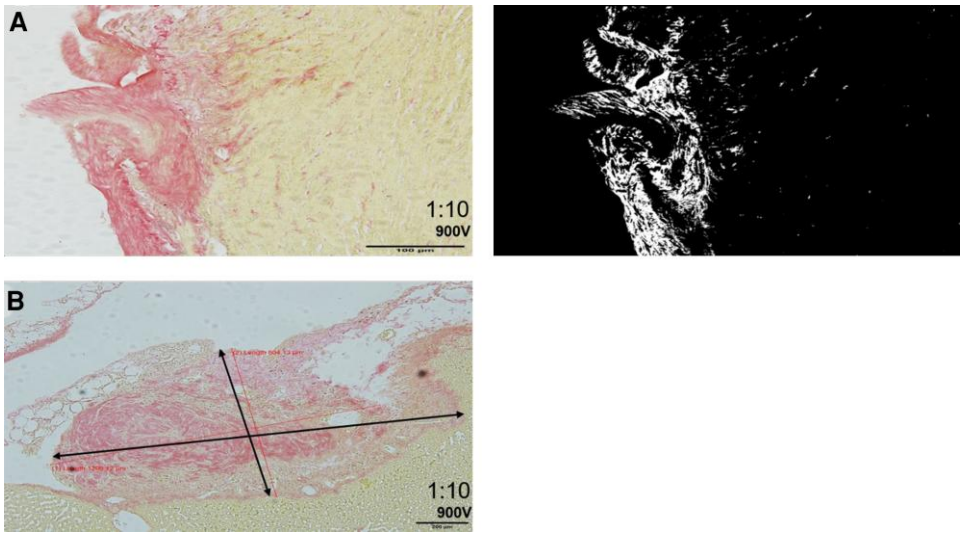

Figure 2 Quantitative evaluation of tissue damage; evaluation of tissue damage by fibrosis measurements as quantified by (*A*) Fiji software (ImageJ®), showing histological sample (left column) of scarred ablated skeletal muscle tissue (fibrosis is stained with red (left side), from the 900 V and after Fiji software analysis (right column, fibrosis is marked in white (left side)) and (*B*) direct measurements of length and width using CellSense Imagine software (Olympus®) on scarred ablated liver tissue, from the 900 V.

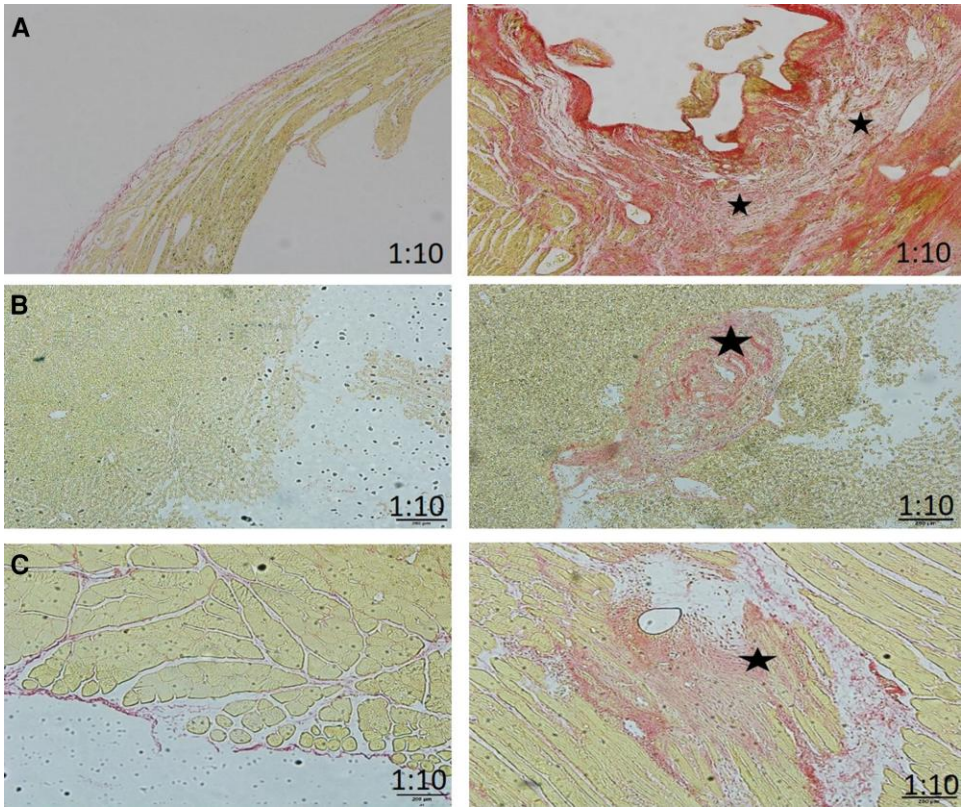

Figure 3 Histological appearance of tissue damage; histology of (*A*) cardiac, (*B*) liver, (*C*) skeletal muscle (*D*) nerve tissues and (*E*) carotid artery. Fibrosis is stained with red after Picrosirius and marked with an asterisk (indicates tissue injury). Scarred ablated tissue from the 900 V protocol group (right column) is compared with the healthy tissue from each organ (left column) showing greater damage to the heart. Carotid artery samples did not demonstrate significant damage in all protocols.

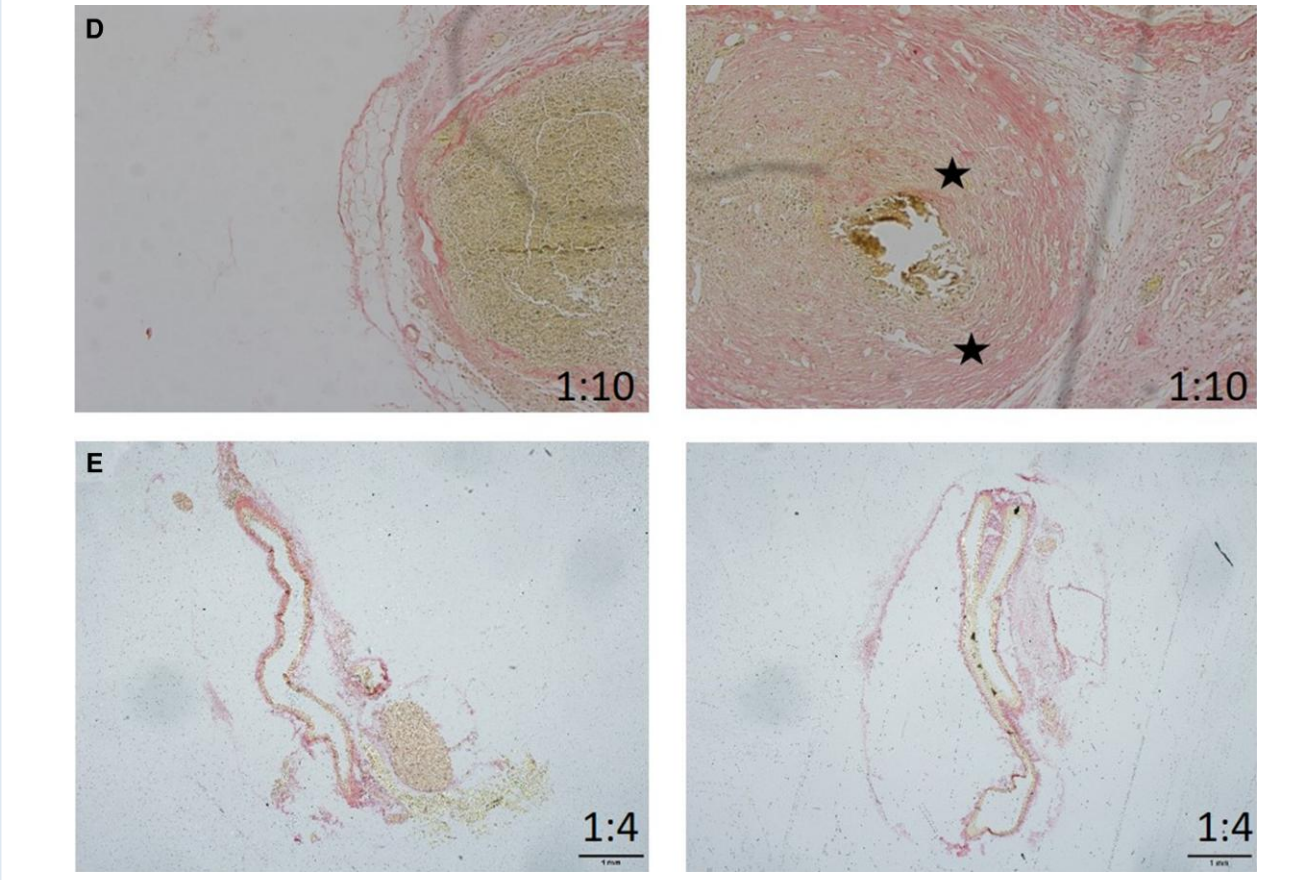

Figure 3 Continued

neural, hepatic, and skeletal muscle tissues. This was most pronounced with the highest voltage protocol. In addition, this study describes in detail the specific electroporation protocols and thresholds that will allow safe ablation of myocardial tissue while sparing adjacent structures.

While PFA use for pulmonary vein isolation and substrate modification is expanding in clinical practice, electroporation pulse protocols are not disclosed by the industry and tissue selectivity remains unestablished. Due to the proximity of the left atrium to surrounding tissues including phrenic nerve, oesophagus and aorta, tissue selectivity of PFA is clinically important. *In vivo* porcine models demonstrated that IRE did not induced histopathologic oesophageal damage as opposed to RFA that exhibited a spectrum of oesophageal lesions.[22–24] Similar findings were obtained evaluating the phrenic nerve[25] and coronary arteries,[19] with no apparent injury in both. Additionally, in recent clinical trials, PFA was shown to spare adjacent tissues while avoiding oesophageal injury following pulmonary vein isolation, as evaluated by cardiac magnetic resonance imaging.[24] Although available data suggests a clinical advantage of PFA over thermal ablation, protocol-specific and threshold-specific data were not fully detailed. In respect to the studies mentioned above, the current study offers specific protocols and tissue thresholds for a selective ablation with minimal collateral damage while maintaining efficient ablation.

Our findings are in line with contemporary data and suggest that HF-IRE is tissue-specific such that cardiac tissue is more susceptible to injury than neural or vascular tissue. In the 900 V protocol, most extensive damage was evident in the myocardium with a significant difference between other tissues as observed by morphometric analysis and by tissue fibrosis ratio. This may imply that at high voltage, cardiac ablation is both more selective and effective with respect to other protocols. In addition, cardiac tissue showed a positive correlation between voltage and extent of damage implying that by adjusting voltage, a desirable ablation could be achieved. In correspondence with previous studies,[26] damage to the carotid artery was not observed in any of the three protocols, while damage to neural tissue was noted only with higher voltages, with two (25%) and one (14%) samples affected in the 600 and 900 V protocols, respectively.

Extracellular characteristics, such as size and nucleus-cytoplasmic ratio, play a role in determining the voltage threshold for which the cell will undergo apoptosis and thus its propensity to electroporation damage.[27,28] Ivey *et al.*[27] studied HF-IRE on glioblastoma tissue. They found that nuclear/cytoplasm ratio rather than cell size, determined the threshold for cell death. The higher was nuclear/cytoplasm ratio, and the lower was the electrical field required to induce apoptosis. This effect was attributed to changes in impedance of the cytoplasm suggesting that cells with smaller volume but higher nuclear/cytoplasm ratio are more prone to HF-IRE ablation. In addition, the study proposed that electroporation is waveform frequency dependent and that short (~1 μs) pulses rather than longer pulses are more effective in inducing of cell death. Other characteristics such as the specific myofibrillar architecture, myocardial gap junctions, and high metabolic activity also contributed the low threshold for IRE and thus its propensity to electroporation damage.[27,28] The relative tolerance of neural or vascular tissues to electroporation in our study could be explained by the presence of a thick connective tissue protecting them by increasing the tissue electrical resistivity.[29] Ben-David *et al.*[28] demonstrated in a porcine model that IRE ablation damage is tissue-specific and depends on tissues conductivity, biochemical properties, and electrode

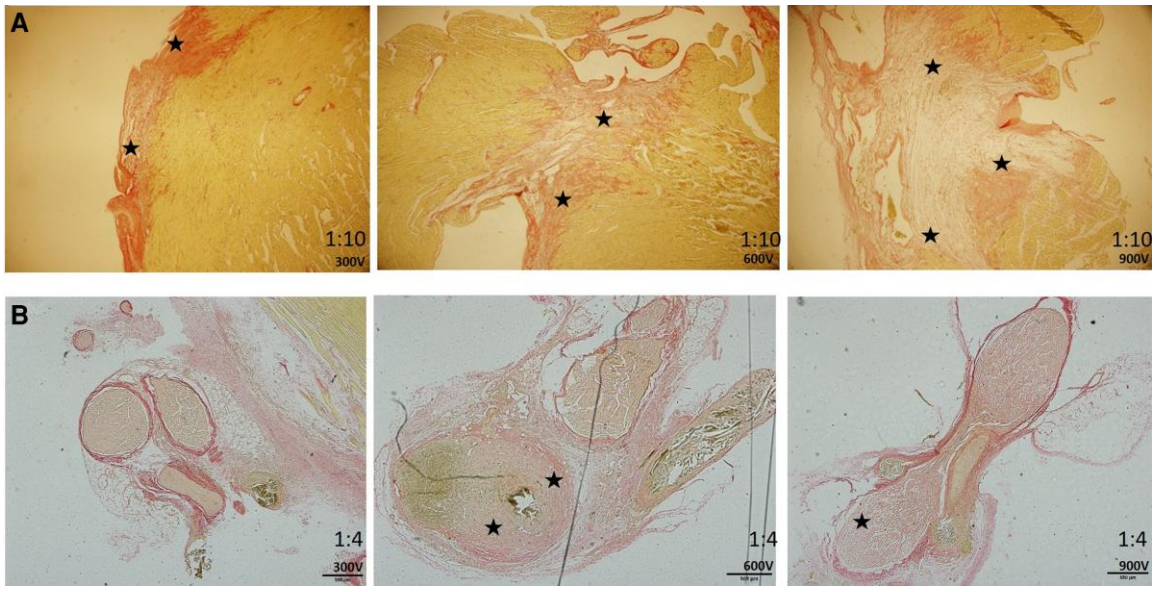

Figure 4 Effect of voltage on tissue damage; histology of (*A*) myocardial tissue and (*B*) nerve tissue after being treated with 300 V protocol (left column), 600 V protocol (middle column) and 900 V protocol (right column) showing a graded effect of voltage in the heart but not in the Sciatic nerve. Fibrosis is stained with red after Picrosirius and marked with an asterisk (indicates tissue injury).

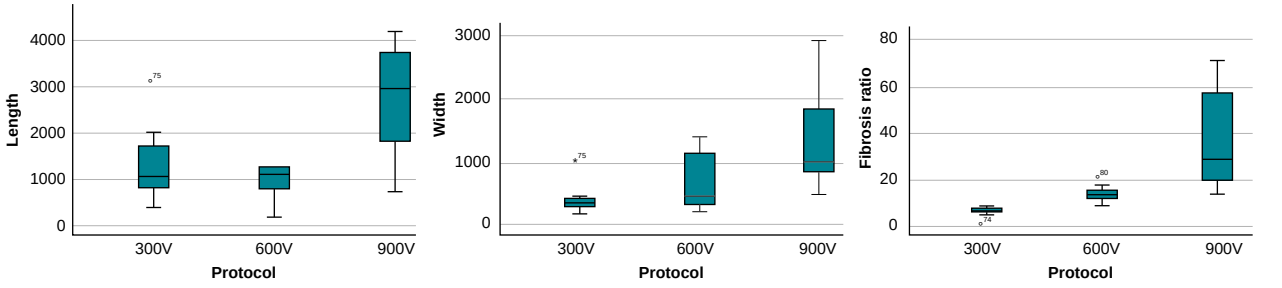

Figure 5 Evaluation of the degree of fibrosis in the heart for different protocols as quantify be length (μM), width (μM) and fibrosis ratio. A comparison between different protocols (300 V vs. 600 V vs. 900 V) for myocardial damage as evaluated by length (μM), width (μM) and fibrosis ratio, showing a positive correlation between voltage and extent of damage in width and fibrosis ratio.

orientation. The study showed that damage to muscle fibres was substantially greater when electrodes were placed exactly parallel to the fibres. Furthermore, the implementation of repetitive IRE pulses to the liver showed decrease in current as opposed to skeletal muscle that showed higher baseline current and increase in current after multiple IRE pulses. This difference was attributed to the sarcoplasmic reticulum of skeletal muscle or extracellular matrix activation. The study also found that staining for cleaved caspase-3 or heat shock protein 70 (HSP-70) in the muscle was negative as opposed to the liver, in which extensive cleaved caspase-3 and limited HSP-70 staining were noted, suggesting different biochemical mechanism for cell death.

The current study failed to show a significant difference in damage between skeletal muscle and liver tissues. These findings could be explained by variation in the orientation of the electrode during the procedure for different tissues, as well as different recovery time during 14 days of follow-up (i.e. faster tissue regeneration in the liver compared with other tissues).[26]

In addition, our findings support the theoretical hypothesis that cardiomyocytes are more prone to damage due to similar properties as skeletal muscle in addition to direct electrical coupling due to gap junctions that increase current transfer between the cells and thus IRE induce damage.

In a recent publication, applying similar methodology as the current study, our group[17] showed that HF-IRE was non-inferior to standard monophasic direct current electroporation with comparable tissue damage yet with minimal muscle contractions. In the current study, following application of 20 bursts, 100 μs burst duration, biphasic square wave with 150 kHz polarity change and a repetition rate of 1 burst/s; most liver, heart and skeletal muscle samples were affected in all protocols with notable damage. In addition, minimal to none muscle contractions were observed after cardiac, carotid and liver ablation and with limited movement of the affected limb after skeletal muscle or sciatic nerve ablation, further supporting our previously reported findings.[17]

Strength and limitations

Our study has several limitations. First, only three protocols were examined using differing amplitudes by using the same repetition rate and

frequency. Second, due to the nature of the study, an objective evaluation of damage with comparison between different tissues with different biophysical properties and recovery time is limited. However, quantification of damage by width, length and fibrosis ratio demonstrated high correspondence between them. Moreover, measurements of length and width were conducted by two different observers, reducing the probability of bias. Third, we used the standard two needle or clamp electrode configuration, therefore our results can only be applied to those configurations. Fourth, we compared between two different configuration with different properties and thus different electrical fields. This limitation was a result of the anatomical differences of the different tissues, requiring a specific configuration to be implemented, in order to maintain a desirable tissue contact and pulse delivery. Fifth, representative waveforms documentation during ablation was only available for cardiac ablation. Lastly, we did not performed a sham procedure in the current study. Nonetheless, previously published studies,[30] implementing similar methodology and electrode configurations, demonstrated the absence of tissue injury after preforming sham procedure. Furthermore, all electroporation protocol included at least one sample without any observable damage, which serves as a shame procedure *de facto*.

Despite these limitation, the current study provides a comprehensive evaluation of five different tissues with more than 300 histological slides analyzed, comparing between three different HF-IRE protocols that were fully disclosed in detail while experimenting with two different electrode configurations with minimal muscle contraction documented during procedures. Moreover, the study offers specific protocols for a selective and efficient ablation.

Conclusion and clinical implications

Electroporation effect is tissue-specific such that myocardium is more prone to electroporation damage compared with hepatic, vascular, and neural tissues. Our results suggest no neural or vascular damage with using a low-amplitude HF-IRE protocol. When planning PFA treatment, protocol details are critical and should be disclosed. By choosing the optimal protocol, safety can be improved and collateral damage to non-myocardial tissue can be minimized. Further investigation is warranted to better identify tissue-specific thresholds.

Supplementary material

Supplementary material is available at *Europace* online.

Acknowledgements

This work was performed in partial fulfilment of Ms. Dvora Grynberg, M.D. Thesis requirements of the Sackler Faculty of Medicine, Tel Aviv University.

Funding

Funded by the Nicholas and Elizabeth Shlezak Super Center for Cardiac Research and Biomedical Engineering at Tel Aviv University.

Conflict of interest**:** None declared.

Data availability

All data including protocols, equipment, histological slides and data base will be fully disclosed upon reasonable request to the corresponding author.

References

1. Go AS, Hylek EM, Phillips KA, Chang Y, Henault LE, Selby JV *et al.* Prevalence of diagnosed atrial fibrillation in adults: national implications for rhythm management and stroke prevention: the AnTicoagulation and Risk Factors in Atrial Fibrillation (ATRIA) study. *JAMA* 2001;**285**:2370–5.
2. Haegeli LM, Calkins H. Catheter ablation of atrial fibrillation: an update. *Eur Heart J* 2014;**35**:2454–9.
3. Calkins H, Hindricks G, Cappato R, Kim Y-H, Saad EB, Aguinaga L *et al.* 2017 HRS/EHRA/ECAS/APHRS/SOLAECE expert consensus statement on catheter and surgical ablation of atrial fibrillation. *Heart Rhythm* 2017;**14**:e275–444.
4. Haïssaguerre M, Jaïs P, Shah DC, Takahashi A, Hocini M, Quiniou G *et al.* Spontaneous initiation of atrial fibrillation by ectopic beats originating in the pulmonary veins. *N Engl J Med* 1998;**339**:659–66.
5. Haegeli LM. Cardiopulse. Percutaneous radiofrequency catheter ablation of atrial fibrillation. *Eur Heart J* 2012;**33**:2625-27.
6. Yuyun MF, Stafford PJ, Sandilands AJ, Samani NJ, André Ng G. The impact of power output during percutaneous catheter radiofrequency ablation for atrial fibrillation on efficacy and safety outcomes: a systematic review. *J Cardiovasc Electrophysiol* 2013;**24**:1216–23.
7. Grubman E, Pavri BB, Lyle S, Reynolds C, Denofrio D, Kocovic DZ. Histopathologic effects of radiofrequency catheter ablation in previously infarcted human myocardium. *J Cardiovasc Electrophysiol* 1999;**10**:336–42.
8. Wittkampf FHM, van Es R, Neven K. Electroporation and its relevance for cardiac catheter ablation. *JACC Clin Electrophysiol* 2018;**4**:977–86.
9. Lee EW, Thai S, Kee ST. Irreversible electroporation: a novel image-guided cancer therapy. *Gut Liver* 2010;**4**:S99–S104.
10. Witt CM, Sugrue A, Padmanabhan D, Vaidya V, Gruba S, Rohl J *et al.* Intrapulmonary vein ablation without stenosis: a novel balloon-based direct current electroporation approach. *J Am Heart Assoc* 2018;**7**.e009575.
11. Livia C, Sugrue A, Witt T, Polkinghorne MD, Maor E, Kapa S *et al.* Elimination of purkinje fibers by electroporation reduces ventricular fibrillation vulnerability. *J Am Heart Assoc* 2018;**7**:e009070.
12. Reddy VY, Koruth J, Jais P, Petru J, Timko F, Skalsky I *et al.* Ablation of atrial fibrillation with pulsed electric fields: an ultra-rapid, tissue-selective modality for cardiac ablation. *JACC Clin Electrophysiol* 2018;**4**:987–95.
13. Koruth J, Kuroki K, Iwasawa J, Enomoto Y, Viswanathan R, Brose R *et al.* Preclinical evaluation of pulsed field ablation: electrophysiological and histological assessment of thoracic vein isolation. *Circ Arrhythm Electrophysiol* 2019;**12**:e007781.
14. Reddy VY, Anic A, Koruth J, Petru J, Funasako M, Minami K *et al.* Pulsed field ablation in patients with persistent atrial fibrillation. *J Am Coll Cardiol* 2020;**76**:1068–80.
15. Ball C, Thomson KR, Kavnoudias H. Irreversible electroporation: a new challenge in "out of operating theater" anesthesia. *Anesth Analg* 2010;**110**:1305–9.
16. Castellví Q, Mercadal B, Moll X, Fondevila D, Andaluz A, Ivorra A. Avoiding neuromuscular stimulation in liver irreversible electroporation using radiofrequency electric fields. *Phys Med Biol* 2018;**63**:035027.
17. Heller E, Garcia-Sanchez T, Moshkovits Y, Rabinovici R, Grynberg D, Segev A *et al.* Comparing high-frequency with monophasic electroporation protocols in an in vivo beating heart model. *JACC Clin Electrophysiol* 2021;**7**:959–64.
18. Rubinsky B, Onik G, Mikus P. Irreversible electroporation: a new ablation modality–clinical implications. *Technol Cancer Res Treat* 2007;**6**:37–48.
19. Du Pré BC, van Driel VJ, van Wessel H, Loh P, Doevendans PA, Goldschmeding R *et al.* Minimal coronary artery damage by myocardial electroporation ablation. *Europace* 2013;**15**:144–9.
20. Laufer S, Ivorra A, Reuter VE, Rubinsky B, Solomon SB. Electrical impedance characterization of normal and cancerous human hepatic tissue. *Physiol Meas* 2010;**31**:995–1009.
21. Maor E, Ivorra A, Leor J, Rubinsky B. The effect of irreversible electroporation on blood vessels. *Technol Cancer Res Treat* 2007;**6**:307–12.
22. Koruth JS, Kuroki K, Kawamura I, Brose R, Viswanathan R, Buck ED *et al.* Pulsed field ablation versus radiofrequency ablation: esophageal injury in a novel porcine model. *Circ Arrhythm Electrophysiol* 2020;**13**:e008303.
23. Neven K, van Es R, van Driel V, van Wessel H, Fidder H, Vink A *et al.* Acute and long-term effects of full-power electroporation ablation directly on the porcine esophagus. *Circ Arrhythm Electrophysiol* 2017;**10**:e004672.
24. Cochet H, Nakatani Y, Sridi-Cheniti S, Cheniti G, Ramirez FD, Nakashima T *et al.* Pulsed field ablation selectively spares the oesophagus during pulmonary vein isolation for atrial fibrillation. *Europace* 2021;**23**:1391–9.
25. van Driel VJHM, Neven K, van Wessel H, Vink A, Doevendans PAFM, Wittkampf FHM. Low vulnerability of the right phrenic nerve to electroporation ablation. *Heart Rhythm* 2015;**12**:1838–44.
26. Rozenblum N, Zeira E, Bulvik B, Gourevitch S, Yotvat H, Galun E *et al.* Radiofrequency ablation: inflammatory changes in the periablative zone can induce global organ effects, including liver regeneration. *Radiology* 2015;**276**:416–25.
27. Ivey JW, Latouche EL, Richards ML, Lesser GJ, Debinski W, Davalos RV *et al.* Enhancing irreversible electroporation by manipulating cellular biophysics with a molecular adjuvant. *Biophys J* 2017;**113**:472–80.
28. Ben-David E, Ahmed M, Faroja M, Moussa M, Wandel A, Sosna J *et al.* Irreversible electroporation: treatment effect is susceptible to local environment and tissue properties. *Radiology* 2013;**269**:738–47.
29. Sances A, Myklebust JB, Larson SJ, Darin JC, Swiontek T, Prieto T *et al.* Experimental electrical injury studies. *J Trauma* 1981;**21**:589–97.
30. Zager Y, Kain D, Landa N, Leor J, Maor E. Optimization of irreversible electroporation protocols for in-vivo myocardial decellularization. *PLoS One* 2016;**11**:e0165475.